Letters

A Strong Misalignment-Tolerance Wireless Power Transfer System Based on Dynamic Diffusion Magnetic Field for Unmanned Aerial Vehicle Applications

Can Zhang, Shuai Wu, *Member, IEEE*, Xichen Liu, *Student Member, IEEE*, Xiuyun Ren, Ziqian Guo, Jinpeng Yu, *Senior Member, IEEE*, and Chunwei Cai, *Member, IEEE*

***Abstract*—The peculiar structure, restricted payload ability, and inevitable landing position deviation of the unmanned aerial vehicles (UAVs) have become the bottleneck, restricting their wireless power transfer (WPT) applications. To overcome these problems, a dynamic diffusion magnetic field, based on the two-phase transmitting circular coils arranged at intervals, is established by the design of the magnetic structure and excitation current phase. At this time, the receiver can be simplified as a rectangular coil and small magnetic core, which only picks up the horizontal magnetic flux to achieve a compact design. Then, the transmitter self-coupling is analyzed and a decoupling transformer is built for the circulation active power feedback. Finally, a UAV WPT prototype is constructed, and the experimental result indicates that it can transfer 286.7 W with a dc–dc efficiency of 80.3%, and maximum fluctuation of output dc current and dc–dc efficiency are only 0.48 A and 2.1% under the UAV dislocation.**

***Index Terms*—Dynamic diffusion magnetic field, unmanned aerial vehicle (UAV), wireless power transfer (WPT).**

I. Introduction

AN UNMANNED aerial vehicle (UAV) is a kind of automatic equipment undertaking power line inspection, delivery, and plant protection [1]. Because the capacity of the onboard battery is insufficient, the endurance time of UAV is limited. The traditional wire recharging or battery replacement requires manual participation, which hinders the UAV's intellectualization. So, based on the characteristic of contactless and charging automation design friendliness [2], wireless power transfer (WPT) has been gradually applied in UAV applications.

The peculiar structure, restricted payload ability, and inevitable landing position deviation of UAV all put forward the novel requirements for WPT technology. To overcome these obstacles, some research works have been made. In [3], a unipolarity coupler with a spiral tube receiving coil and a nonlinear parity-time-symmetric model is proposed. Although the transfer power and efficiency of the system reach 10 W and 93.6% separately showing strong misalignment tolerance, electromagnetic safety is hard to guarantee in high-power occasions, and the original structure of a UAV is destroyed. Bie et al. [4] adopted a solenoid structure covering on the bottom of the landing gear as a receiver in bipolar mode to achieve 200 W power transmission with the dc–dc efficiency of 90%. However, the experimental prototype is weak in lateral misalignment. So, a strong antimisalignment WPT system for UAVs with enough power transfer, good structure adaptability, and safe electric-flux working area is urgent.

The changes in electrical parameters caused by the misalignment of the coupler can be attributed to the instability of the magnetic flux receiving. Therefore, some scholars have studied the coupling mechanism from the perspective of emitting a uniform magnetic field or picking up omnidirectional magnetic flux. A large-to-small asymmetric coil is introduced to improve misalignment tolerance in [5]. While the structure dramatically extends the range of magnetic fields, its dimensional differential design leads to a "peak" distribution of emission magnetic showing with a strong center and weak edge. To solve the problem, an additional transmitting coil wound in series and reverse is used to decrease the center magnetic field [6]. In this case, the magnetic field is distributed in the shape of a straw hat, which offers a uniform flux. However, there is a large amount of magnetic flux not involved in the effective coupling, leading to low efficiency and large electromagnetic interference. So, a multicoil structure is proposed to improve effective charging space in [7]. It applies four switchable transmitters and one receiver to compose a coupler for achieving selective activation coils. Besides, the parallel transmission coil matrix structure is proposed in [8]. Based on the receiving coil's position detection method, part of the transmitting coil is quickly excited to ensure the system's efficient operation. However, the additional coils and complex

Manuscript received 29 March 2024; revised 9 May 2024 and 14 June 2024; accepted 8 July 2024. Date of publication 11 July 2024; date of current version 11 September 2024. This work was supported in part by the National Natural Science Foundation of China under Grant 52177002, in part by the Major Scientific and Technological Innovation Project of Shandong Province of China under Grant 2022ZLGX04, and in part by the National Science and Technology Innovation 2030 under Grant 2022ZD0116409. *(Corresponding author: Shuai Wu.)*

Can Zhang, Shuai Wu, Xichen Liu, Xiuyun Ren, Ziqian Guo, and Chunwei Cai are with the School of New Energy, Harbin Institute of Technology, Weihai 264209, China, and also with the Key Laboratory of Cross-Domain Synergy and Comprehensive Support for Unmanned Marine Systems, Ministry of Industry and Information Technology, Weihai 264209, China (e-mail: 2021212568@stu.hit.edu.cn; wushuai@hit.edu.cn; 230155@hit.stu.edu.cn; renxiuyun@hit.edu.cn; 2022212530@stu.hit.edu.cn; caichunwei@hit.edu.cn).

Jinpeng Yu is with the School of Automation, Qingdao University, Qingdao 266071, China (e-mail: yjp1109@qdu.edu.cn).

Color versions of one or more figures in this article are available at https://doi.org/10.1109/TPEL.2024.3426609.

Digital Object Identifier 10.1109/TPEL.2024.3426609

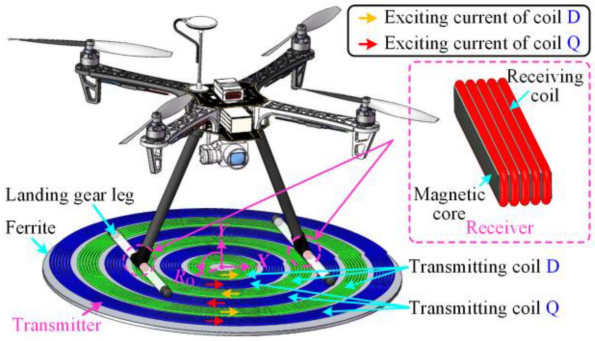

Fig. 1. General overview of the proposed magnetic coupler.

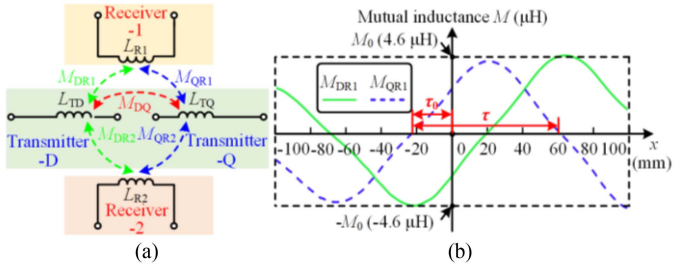

Fig. 2. (a) Equivalent circuit model of the coupler. (b) Mutual inductance performance changes with the distance x from UAV's center to transmitter's center when the receiver rotates 0°.

controller design have limited the applications. Except for the transmitter, an omnidirectional magnetic flux receiver also benefits the stable power transfer for UAVs. Wu et al. [9] proposed a magnetic coupler with one circular target transmitting coil and two receivers. By integrating two orthogonal receiving coils into one receiver, the parallel- and vertical-flux can be picked up complementarily showing better output stability under angle and horizontal misalignments. However, the output fluctuation still exists in 20% and the improved number of coils hinders the lightweight design of receivers.

Constructing a dynamic magnetic field in the desired space is also an alternative solution for a high charging degree of freedom. In [10] and [11], a two-phase transmitter is adopted to generate a 2-D rotating magnetic field so that the device can be freely charged over a wide-range space. Inspired by the works of [9], [10], and [11], a dynamic diffusion magnetic field is constructed to improve the antimisalignment ability and decrease the receiver complexity based on the design of the magnetic structure and excitation current phase. The magnetic distribution is then verified via ANSYS Maxwell simulations. A decoupling circuit is given to further restrain the self-coupling of the transmitting coils and a strong misalignment-tolerance UAV WPT system is constructed to validate the proposal. The main contributions of this letter are summarized as follows.

1) A miniaturized receiver based on horizontal magnetic flux is implemented.
2) A uniform dynamic diffusion magnetic field is constructed for a high charging degree of freedom.
3) A self-coupling impact relief method has been proposed to improve efficiency.

II. Magnetic Structure Proposal and Analysis

A. Magnetic Structure With Compact Receiver

To ensure the output stability under misalignment, a dynamic diffusion magnetic field with the same amplitude is constructed by the design of the magnetic structure and excitation current phase. As for the magnetic structure design, an integral structure of the proposed magnetic coupler, which consists of one transmitter and two receivers, is depicted in Fig. 1. On the transmitting side, the transmitting coil D, transmitting coil Q, and the ferrite located in the back construct the transmitter. Each transmitting coil contains three concentric subcoils with a radius of arithmetic arrangement in reverse series, respectively. Meanwhile, the subcoils of the two groups of transmitting coils are arranged at intervals. Therefore, the exciting current flows of any two adjacent transmitting coils are opposite, producing the alternate complementary distribution of horizontal magnetic flux in the transmitter plane. Based on that, a compact receiver with a cuboid magnetic core and receiving coil capable of picking up only horizontal flux is proposed. Its size is small to be mounted inside the hollow transverse bar at the bottom of the landing gear, which adapts to the structure of UAVs and reduces the occupied space. Meanwhile, two same receivers are set at both sides of UAV to ensure the power transfer capacity. It should be mentioned that the number of transmitting coils is not fixed, and the number of coils can be increased or decreased according to the actual misalignment demand range.

B. Diffusing Magnetic Flux Construction to Suppress Output Fluctuations

Fig. 2(a) shows the equivalent circuit model of the magnetic coupler. L_{TD} and L_{TQ} are the self-inductance of the transmitting coils, L_{R1} and L_{R2} are the self-inductance of the receiving coils, M_{DR1}, M_{QR1}, M_{DR2}, and M_{QR2} are the mutual-inductance between the transmitting and receiving coils, and M_{DQ} is the mutual inductance between the two transmitting coils. Because the two energy pickup channels being independent of each other, one receiver can be taken as an example to elucidate the operation principle of the proposal. As shown in Fig. 2(b), the mutual inductance between the transmitting and receiving coils, which is measured by an impedance analyzer, presents a sine-cosine distribution, and M_{DR1} and M_{QR1} can be approximated as (1). τ is two times the width of the transmitting coil windings, and τ_0 is the translation length of the mutual inductance curve. Although superimposing the coupling effect of two sets of transmitting coils on the receiving coils can eliminate the energy zero zone, the output fluctuation is still significant.

$$\begin{cases} M_{\mathrm{DR1}}(x) = -M_0 \cos\left(2\pi \bullet \frac{x}{2\tau} + \tau_0\right), \\ \quad x \in [-100\ \mathrm{mm}, 100\ \mathrm{mm}] \\ M_{\mathrm{QR1}}(x) = M_0 \sin\left(2\pi \bullet \frac{x}{2\tau} + \tau_0\right), \\ \quad x \in [-100\ \mathrm{mm}, 100\ \mathrm{mm}] \end{cases} \tag{1}$$

where M_0 denotes the amplitude of the mutual inductance.

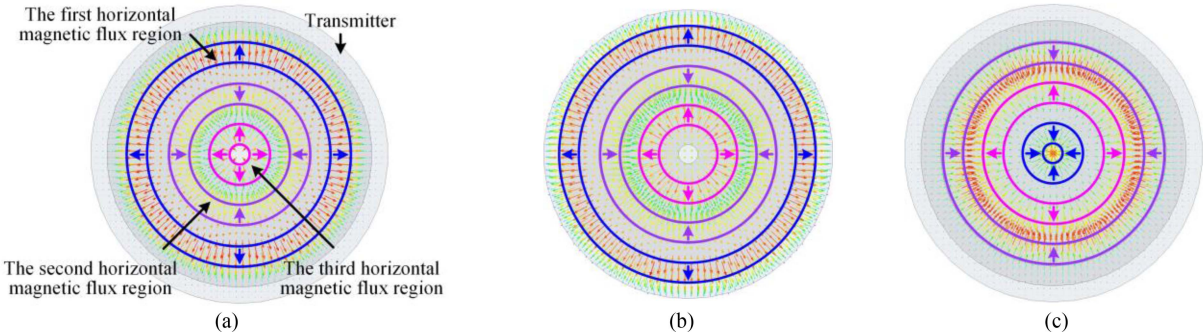

Fig. 3. Circular dynamic diffusion magnetic field. (a) $\omega t = 0$. (b) $\omega t = \pi/2$. (c) $\omega t = \pi$.

Considering the induced voltage of the receiver that depends not only on the mutual inductance but on the excitation current, an excited mode with the same amplifies and phase difference of 90° is applied in the transmitter to achieve stable output. In this case, the magnetic flux distribution Φ_{DR1} and Φ_{QR1} generated by the transmitting coil D and coil Q is expressed as

$$\begin{cases} \Phi_{\mathrm{DR1}}(t) = -\Phi_{\mathrm{TR0}} \cos\left(\frac{\pi x}{\tau} + \tau_0\right) \cos(\omega t) \\ \Phi_{\mathrm{QR1}}(t) = \Phi_{\mathrm{TR0}} \sin\left(\frac{\pi x}{\tau} + \tau_0\right) \cos\left(\omega t + \frac{\pi}{2}\right) \end{cases} \tag{2}$$

where ω is the angular frequency, and Φ_{TR0} refers to the amplitude of magnetic flux.

Hence, the superimposed magnetic flux and induced voltage of the receiver are obtained in (3) and (4). It can be obtained that the amplitudes of the interlinked magnetic flux and the induced voltage are Φ_{TR0} and $\omega N_{\mathrm{R}} \Phi_{\mathrm{TR0}}$, respectively. The offset distance x only affects the phase ($\pi x/\tau + \tau_0$) of the interlinked magnetic flux and the induced voltage, while the amplitudes remain constant, which provides a prerequisite for stable output under misalignment.

$$\Phi(t) = \Phi_{\mathrm{DR1}}(t) + \Phi_{\mathrm{QR1}}(t) = -\Phi_{\mathrm{TR0}} \cos\left(\omega t - \frac{\pi x}{\tau} - \tau_0\right) \tag{3}$$

$$u_{\mathrm{R1}}(t) = -\mathrm{j}\omega N_{\mathrm{R}} \Phi_{\mathrm{TR0}} \cos\left(\omega t - \frac{\pi x}{\tau} - \tau_0\right). \tag{4}$$

To validate the previous analysis, the magnetic flux varied as time is simulated by ANSYS Maxwell and illustrated in Fig. 3. It can be pointed out that the emission magnetic field continues to spread dynamically from the center of the transmitter to the surroundings, conforming to the sine law. So, the impulse of the magnetic flux at each position in a period is equal, providing the foundation for achieving stable output.

III. System Circuit Topology Design

A. Analysis and Elimination of Self-Coupling Effects

There is not only mutual coupling between the transmitting coils and receiving coils, but also self-coupling between the two sets of transmitting coils. To investigate the impact of self-coupling between the transmitting coils, the equivalent model of the transmitter is established, as shown in Fig. 4.

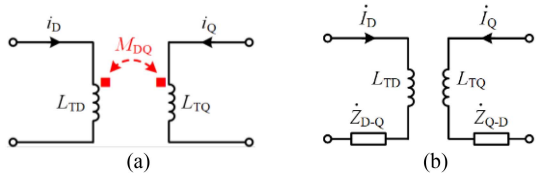

Fig. 4. Circuit model of the transmitter with self-coupling. (a) Mutual inductance model. (b) Reflecting impedance equivalent model.

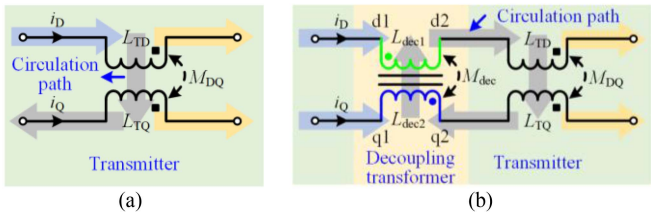

Fig. 5. (a) Active power transfer circulation path. (b) Decoupling principle.

$\dot{Z}_{\mathrm{Q-D}}$ and $\dot{Z}_{\mathrm{D-Q}}$, respectively, represent the impact of transmitting coil D on transmitting coil Q and the impact of transmitting coil Q on transmitting coil D. According to Fig. 4, the self-coupling reflection impedance model of the transmitter can be obtained as (5). The currents $\dot{I}_{\mathrm{D}}$ and $\dot{I}_{\mathrm{Q}}$ involved in the equation can be found in the following text:

$$\dot{Z}_{\mathrm{Q-D}} = \frac{\mathrm{j}\omega M_{\mathrm{DQ}} \dot{I}_{\mathrm{Q}}}{\dot{I}_{\mathrm{D}}} = \omega M_{\mathrm{DQ}}, \dot{Z}_{\mathrm{D-Q}} = \frac{\mathrm{j}\omega M_{\mathrm{DQ}} \dot{I}_{\mathrm{D}}}{\dot{I}_{\mathrm{Q}}} = -\omega M_{\mathrm{DQ}}. \tag{5}$$

According to (5), the transmitting coil D will transmit active power with a value of $\omega M_{\mathrm{DQ}} I_{\mathrm{D}}$ to the transmitting coil Q, causing the residual active power flows reversely to the inverting source shown in Fig. 5(a). The behavior will not only induce additional loss but also increase the capacity of inverter.

To eliminate the effect of the transmitting coils self-coupling, a decoupling transformer is designed and its working principle is given in Fig. 5(b). The primary side (L_{dec1}) is connected to the transmitting coil D and the secondary side (L_{dec1}) is connected to the transmitting coil Q, respectively, to transfer active power back. The core parameter design principle of the decoupling transformer is to ensure that the mutual inductance M_{dec} is equal

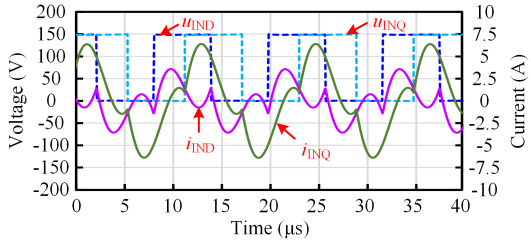

Fig. 6. Simulation of the inverter output after adding a decoupling transformer.

to M_{DQ} of the transmitter guaranteeing the circulation active power feedback. It should be mentioned that the generation of L_{dec1} and L_{dec2} is related to opening the gap of the magnetic core (to avoid saturation), and it is expected to minimize these two self-inductance values as much as possible. In addition, when designing compensation circuits, it is necessary to compensate for these two self-inductance effects.

The inverter output after adding a decoupling transformer is simulated by PSpice, depicted in Fig. 6. It should be clarified that the time starting point in the figure is the data statistics starting point, not the simulation starting point. It shows that the output voltage u_{IND} (u_{INQ}) and current i_{IND} (i_{INQ}) of the D-phase or Q-phase inverter are approximately in phase [12], indicating that the active power flowing back to the inverter is successfully prevented. At this time, the inverter's efficiency and stability can be improved.

B. System Topology Design and Transmission Performance Analysis

The circuit topology of the proposed UAV WPT system is shown in Fig. 7(a). On the transmitting side, the inductance–capacitance–capacitance (*LCC*)-compensated circuit composed by L_x, C_{x1}, and C_{x2} (x = Q, D) and designed decoupling transformer are built to provide constant excitation current for the transmitter. Meanwhile, a two-phase two-leg (leg-D and leg-Q) inverter is used to provide two independent inverting sources (u_{IND} and u_{INQ}), and u_{INQ} is $\pi/2$ lag of u_{IND}. The gate drive signals and output voltages of the two-phase inverter are plotted in Fig. 7(b), which is different from the traditional H-bridge inverter control method. It also should be noted that the inverter controlled by this method is suitable for *LCC* compensation, but not for *LCL*, as capacitor can isolate the dc current component. Taking the exciting current of transmitting coil D as the phase reference, the excitation voltage of two transmission channels can be obtained as

$$\dot{U}_{IND} = \frac{\sqrt{2}}{\pi} U_{DC} e^{j\frac{\pi}{2}}, \dot{U}_{INQ} = \frac{\sqrt{2}}{\pi} U_{DC} e^{j\pi}. \tag{6}$$

On the receiving side, the series–parallel (SP) consisting of C_{R11}, C_{R12}, C_{R21}, and C_{R22} is applied to obtain constant output current. Then, the power from the multiple pickup channels can be superposed in parallel through rectifiers for the UAV energy supply. Since two receivers work independently, one of them is modeled and studied as an example for simplifying the analysis complexity. Then, the system equivalent circuit model is given in Fig. 7(c).

Under the angular frequency ω, the parameters of the system components should satisfy the following equation:

$$\begin{cases} \omega = \frac{1}{\sqrt{L_D C_{D1}}} = \frac{1}{\sqrt{L_Q C_{Q1}}} = \frac{1}{\sqrt{(L_{R1} - \frac{1}{\omega^2 C_{R11}}) C_{R21}}} \\ L_D = L_Q = L_{TD} + L_{dec1} - \frac{1}{\omega^2 C_{D2}} = L_{TQ} + L_{dec2} \\ \quad - \frac{1}{\omega^2 C_{Q2}} = L. \end{cases} \tag{7}$$

The *LCC* compensation topology of cascaded voltage source inverter has a constant current output [12], and the excitation current of two sets of transmitting coils can be obtained as

$$\dot{I}_D = \frac{\dot{U}_{IND}}{j\omega L_D} = \frac{\sqrt{2}}{\pi} \frac{U_{DC}}{\omega L_D}, \dot{I}_Q = \frac{\dot{U}_{INQ}}{j\omega L_Q} = j\frac{\sqrt{2}}{\pi} \frac{U_{DC}}{\omega L_Q}. \tag{8}$$

The induced voltage of the receiver-1 can be described by

$$\begin{aligned} \dot{U}_{R1} &= j\omega M_{DR1} \dot{I}_D + j\omega M_{QR1} \dot{I}_Q \\ &= \frac{\sqrt{2}}{\pi} \frac{M_0 U_{DC}}{L} \left[\cos\left(\frac{\pi x}{\tau} + \tau_0\right) + j \sin\left(\frac{\pi x}{\tau} + \tau_0\right) \right]. \end{aligned} \tag{9}$$

Further, the output current of the first receiving channel can be derived as follows:

$$\dot{I}_{out1} = \frac{\sqrt{2}}{\pi} \frac{M_0 U_{DC} \omega C_{R21}}{L} \left[\cos\left(\frac{\pi x}{\tau} + \tau_0\right) + j \sin\left(\frac{\pi x}{\tau} + \tau_0\right) \right]. \tag{10}$$

The root-means-square (rms) value of $\dot{I}_{out1}$ is

$$I_{out1} = \frac{M_0 U_{DC} \omega C_{R21}}{\pi L}. \tag{11}$$

Correspondingly, the rms value of the output current of the second receiving channel (i_{out2}) can also be obtained as

$$I_{out2} = \frac{M_0 U_{DC} \omega C_{R22}}{\pi L}. \tag{12}$$

The superimposed output current model of the system can be obtained as shown in (7), where $C_{R2} = C_{R21} = C_{R22}$. Since the amplitude of mutual inductance, shown in Fig. 2, is constant, the stable system output is finally achieved. Namely, the whole system output characteristic is stable, possessing strong capability of antimisalignment under the cooperation of the magnetic structure and excitation time.

$$I_O = \frac{\pi}{2\sqrt{2}} (I_{out1} + I_{out2}) = \frac{M_0 U_{DC} \omega C_{R2}}{\sqrt{2} L}. \tag{13}$$

IV. Experimental Verification

A. Experimental Prototype and Power Transmission

In order to verify the proposal, a UAV WPT prototype is established, as shown in Fig. 8. The outer diameter of the transmitting coil is 600 mm, and a 5-mm thick ferrite core is placed at the back of the transmitting coil. In addition, in the receiving side, there is a 90 mm ×15 mm × 5 mm ferrite core, which is added to each receiving coil. The weight of a single receiver is 77.4 g. The other key parameters are listed in Table I.

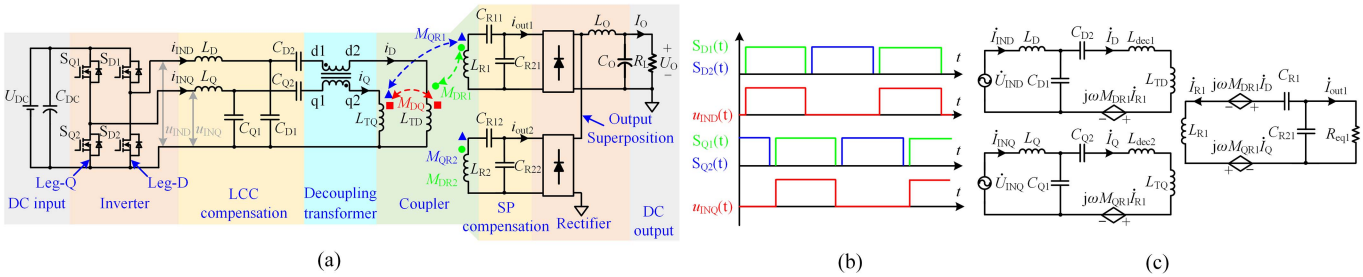

Fig. 7. (a) UAV WPT circuit. (b) Gate drive signals and output voltages of the two-phase inverter. (c) System equivalent circuit model.

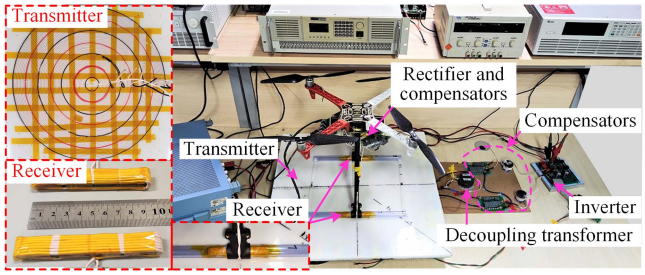

Fig. 8. Experimental prototype.

TABLE I
PARAMETERS OF UAV WPT PROTOTYPE

Parameters	Value	Parameters	Value
U_{DC}	150 V	L_D (L_Q)	19.6 μH
f	85 kHz	C_{D1} (C_{Q1})	176 nF
L_{TD}	137.2 μH	C_{D2} (C_{Q2})	20.6 nF(19.4 nF)
L_{TQ}	179.5 μH	C_{R11}(C_{R12})	340 nF
L_{R1}(L_{R2})	21.95 μH	C_{R21}(C_{R22})	303 nF
M_{DQ}	30 μH	L_{dec1}(L_{dec2})	56.8 μH(23.1 μH)
R_L	15 Ω	Receiver weight	77.4 g(single)

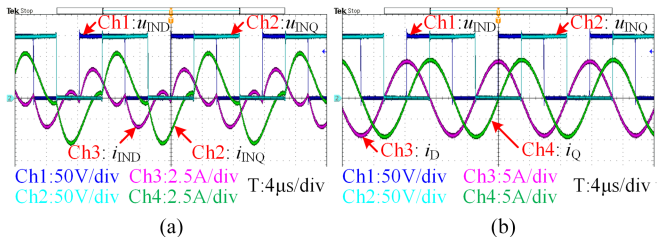

Fig. 9. (a) Output voltages and currents waveform of inverter. (b) Output voltages of inverter and input currents of transmitting coils waveform.

B. System Performance Versus Misalignments

The experimental waveforms are measured in Fig. 9. The output voltage u_{IND} (u_{INQ}) and output current i_{IND} (i_{INQ}) are in phase, achieving the transmitting decoupling in Fig. 9(a). Also, the input current of transmitting coil D exceeds the phase of input current of transmitting coil Q by 90° with the same amplitude in Fig. 9(b), which meets the condition of dynamic diffusion magnetic field. By comparing Figs. 6 and 9, it can be found that the simulation and experimental waveforms are

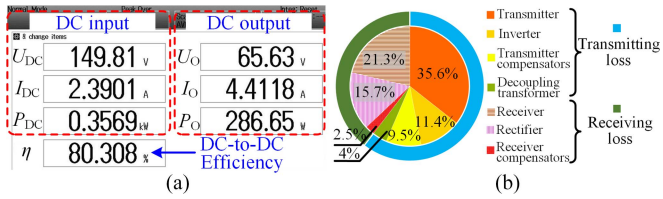

Fig. 10. (a) System input and output power. (b) Distribution of system losses.

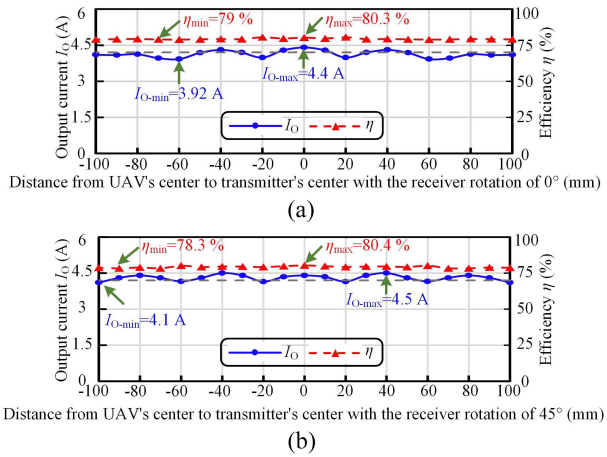

Fig. 11. (a) Antimisalignment performance when rotating 0°. (b) Antimisalignment performance when rotating 45°.

basically consistent, and there are slight deviations in amplitude and phase that may be affected by parameter deviations and parasitic parameters of the circuit components in the experiment prototype.

The system power transfer ability and loss distribution are measured in Fig. 10. It shows that the output power reaches 286.7 W with a dc–dc efficiency of 80.3%, and the loss can mainly be attributed to the magnetic coupler because of the low magnetic coupling coefficient caused by the small receiver.

To validate the strong antimisalignment ability of the proposed system, the output current I_O and system efficiency η against misalignment are tested in Fig. 11. The result indicates that the maximum fluctuation of I_O and η are only 0.48 A and 2.1%, showing the advantages of output stability against misalignment.

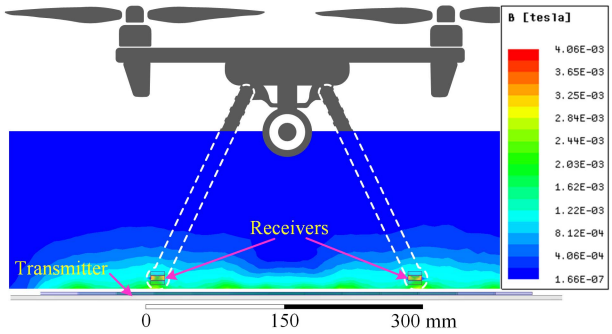

Fig. 12. Magnetic flux density distribution on a cross section of the proposed magnetic coupler.

C. Magnetic Flux Density Distribution

The magnetic flux density distribution of the proposed magnetic coupler is obtained using ANSYS Maxwell, as shown in Fig. 12. It can be observed that the main magnetic flux is concentrated near the transmitter platform, which has a positive effect on reducing leakage magnetic interference to UAV body.

V. Conclusion

This letter proposes a strong misalignment-tolerance WPT system with the dynamic diffusion magnetic field and compact receiver for achieving the omnidirectional charging for UAV. Besides, a decoupling transformer is proposed to eliminate the self-coupling of the transmitting coils. Then, an *LCC*-SP-compensated topology is adjusted to obtain constant current under resonant frequency, showing unaffected by the offset distance. Finally, a practical prototype with 286 W and the efficiency of 80.3% is built to validate the proposal. The experimental result indicates that the idea can be well applied for the UAV wireless charging occasion.

References

[1] H. Shen, D. Lin, and T. Song, "Object detection deployed on UAVs for oblique images by fusing IMU information," *IEEE Geosci. Remote Sens. Lett.*, vol. 19, 2022, Art. no. 6505305, doi: 10.1109/LGRS.2022.3141109.

[2] C. Cai et al., "Optical Fiber composite winding for in situ thermal monitoring of transmitter magnetic mechanism in long-track DWPT systems," *IEEE Trans. Instrum. Meas.*, vol. 73, 2024, Art. no. 9000604, doi: 10.1109/TIM.2023.3329107.

[3] J. Zhou, B. Zhang, W. Xiao, D. Qiu, and Y. Chen, "Nonlinear parity-time-symmetric model for constant efficiency wireless power transfer: Application to a drone-in-flight wireless charging platform," *IEEE Trans. Ind. Electron.*, vol. 66, no. 5, pp. 4097–4107, May 2019, doi: 10.1109/TIE.2018.2864515.

[4] Z. Bie, J. Zhang, K. Song, D. Wang, and C. Zhu, "A free-rotation asymmetric magnetic coupling structure of UAV wireless charging platform with conformal pickup," *IEEE Trans. Ind. Electron.*, vol. 69, no. 10, pp. 10154–10161, Oct. 2022, doi: 10.1109/TIE.2022.3165297.

[5] H. Zhang, Y. Chen, C. -H. Jo, S. -J. Park, and D. -H. Kim, "DC-link and switched capacitor control for varying coupling conditions in inductive power transfer system for unmanned aerial vehicles," *IEEE Trans. Power Electron.*, vol. 36, no. 5, pp. 5108–5120, May 2021, doi: 10.1109/TPEL.2020.3032155.

[6] Y. Chen, R. Mai, Y. Zhang, M. Li, and Z. He, "Improving misalignment tolerance for IPT system using a third-coil," *IEEE Trans. Power Electron.*, vol. 34, no. 4, pp. 3009–3013, Apr. 2019, doi: 10.1109/TPEL.2018.2867919.

[7] C. Cai, J. Wang, H. Nie, P. Zhang, Z. Lin, and Y. -G. Zhou, "Effective-configuration WPT systems for drones charging area extension featuring quasi-uniform magnetic coupling," *IEEE Trans. Transp. Electrific.*, vol. 6, no. 3, pp. 920–934, Sep. 2020, doi: 10.1109/TTE.2020.2995733.

[8] J. Li, F. Yin, L. Wang, B. Cui, and D. Yang, "Electromagnetic induction position sensor applied to anti-misalignment wireless charging for UAVs," *IEEE Sensors J.*, vol. 20, no. 1, pp. 515–524, Jan. 2020, doi: 10.1109/JSEN.2019.2940925.

[9] S. Wu, C. Cai, X. Liu, W. Chai, and S. Yang, "Compact and free-positioning omnidirectional wireless power transfer system for unmanned aerial vehicle charging applications," *IEEE Trans. Power Electron.*, vol. 37, no. 8, pp. 8790–8794, Aug. 2022, doi: 10.1109/TPEL.2022.3158610.

[10] E. S. Lee, D. Kim, and S. Y. Jeong, "Triangular DQ tx coils of wireless EV chargers for large misalignment tolerances," *IEEE Trans. Veh. Technol.*, vol. 72, no. 11, pp. 14179–14188, Nov. 2023, doi: 10.1109/TVT.2023.3288553.

[11] E. S. Lee, Y. H. Sohn, B. G. Choi, S. H. Han, and C. T. Rim, "A modularized IPT with magnetic shielding for a wide-range ubiquitous wi-power zone," *IEEE Trans. Power Electron.*, vol. 33, no. 11, pp. 9669–9690, Nov. 2018, doi: 10.1109/TPEL.2017.2789201.

[12] Z. Pantic, S. Bai, and S. M. Lukic, "ZCS LCC-compensated resonant inverter for inductive-power-transfer application," *IEEE Trans. Ind. Electron.*, vol. 58, no. 8, pp. 3500–3510, Aug. 2011, doi: 10.1109/TIE.2010.2081954.